

Mapping Brain-Behavior Correlations in Autism Using Heat Kernel Smoothing

Moo K. Chung^{a,b,d}, Kim M. Dalton^b, Daniel J. Kelley^b, Richard J. Davidson^{b,c}

^a*Department of Biostatistics and Medical Informatics,*

^b*Waisman Laboratory for Brain Imaging and Behavior,*

^c*Department of Psychology and Psychiatry,*

University of Wisconsin, Madison, WI 53705, USA

^d*Department of Brain and Cognitive Sciences, Seoul National University, Korea*

Abstract

This paper presents a streamlined image analysis framework for correlating behavioral measures to anatomical measures on the cortex and detecting the regions of abnormal brain-behavior correlates. We correlated a facial emotion discrimination task score and its response time to cortical thickness measurements in a group of high functioning autistic subjects. Many previous correlation studies in brain imaging neglect to account for unwanted age effect and other variables and the subsequent statistical parametric maps may report spurious results. We demonstrate that the partial correlation mapping strategy proposed here can remove the effect of age and global cortical area difference effectively while localizing the regions of high correlation difference. The advantage of the proposed correlation mapping strategy over the general linear model framework is that we can directly visualize more intuitive correlation measures across the cortex in each group.

Keywords: Cortical thickness, heat kernel, diffusion smoothing, partial correlation, autism

1. Introduction

Pearson's product-moment correlation (Fisher, 1915), in short simple correlation, has widely been used as a simple index for measuring dependency

Email address: mkchung@wisc.edu (Moo K. Chung)

and the linear relationship between two variables. In human brain mapping research, it has been mainly used to map out functional or anatomical connectivity (Friston et al., 1993; Horwitz et al., 1996; Friston et al., 1996; Cao and Worsley, 1998; Worsley et al., 2005). In this framework, correlations between pairs of voxels are computed and thresholded via the random field theory to reveal the statistically significant regions of connectivity by testing the existence of correlation ρ on the template cortex $\partial\Omega$:

$$H_0 : \rho(p) = 0 \text{ for all } p \in \partial\Omega \text{ vs. } H_1 : \rho(p) \neq 0 \text{ for some } p \in \partial\Omega. \quad (1)$$

In a different setting, Thompson et al. (2001) used the correlation between genetic factors and the amount of gray matter on the cortex via a linear model in mapping out the regions of genetic influence. Our use of correlation is somewhat similar to Thompson et al. (2001) in that we correlate anatomical index to non-anatomical index on the cortex. In this study, we map out the dependency of behavioral measures to an anatomical measure spatially over the cortex and localize the regions of abnormal correlation difference between groups. To remove unwanted covariates like age and total brain size difference, we introduce the concept of *partial correlation coefficient*, in short partial correlation. Chung et al. (2004; 2005) has already demonstrated the need for removing the effect of age and global brain size difference in morphometric analyses so it is crucial to use partial correlation rather than the usual simple correlation in our study. Although our correlation mapping strategy can be formulated in terms of a general linear model (GLM) as in the case of Thompson et al. (2001), our unified approach will provide a more intuitive alternative that is visually comprehensive.

As an application, we applied our method in characterizing abnormal brain-behavior correlation in autism. We correlated two behavioral measures with the anatomical measure, *cortical thickness*. The cortical thickness measures the thickness of the gray matter shell bounded by the both outer and inner cortical surfaces (MacDonald et al., 2000; Chung et al., 2003; Chung et al., 2005). The first behavioral measure is the emotional face recognition task score. The task score counts the number of correct responses when judging whether a subject is viewing an emotional (happy, fear and anger) or neutral face (Dalton et al., 2005). The second behavioral measure is the time required to produce a response. The response time is measured in ms. Each behavioral measure was correlated with the cortical thickness measure at each point on the cortex for the both autistic and control groups, and a

statistical test was performed to determine the regions of differing correlation pattern between groups. This study is a continuation of the series of multifaceted studies in the Waisman laboratory for brain imaging and behavior characterizing the autistic, structural, functional, and behavioral phenotypes (Chung et al., 2004; Chung et al., 2005; Dalton et al., 2005).

2. Preliminary

Let $Y = (Y_1, Y_2)$ be two variables of interests and $X = (X_1, \dots, X_p)$ be a row vector of variables that should be removed in a data analysis. For instance, we may let Y_1 be the cortical thickness, Y_2 be the response time, and X_1 and X_2 be the age and total surface area respectively. The covariance matrix of $(Y, X)'$ is denoted by

$$\mathbb{V}(Y, X)' = \begin{pmatrix} \Sigma_{YY} & \Sigma_{YX} \\ \Sigma_{XY} & \Sigma_{XX} \end{pmatrix} \quad (2)$$

Note Σ_{XY} is the cross-covariance matrix of X and Y . Σ_{YX} and Σ_{XX} are defined similarly. Then the partial covariance of Y given X is

$$\Sigma_{YY} - \Sigma_{YX}\Sigma_{XX}^{-1}\Sigma_{XY} = (\sigma_{ij}).$$

The *partial correlation* $\rho_{Y_i, Y_j|X}$ is the correlation between variables Y_i and Y_j while removing the effect of variables X and it is defined as

$$\rho_{Y_i, Y_j|X} = \frac{\sigma_{ij}}{\sqrt{\sigma_{ii}\sigma_{jj}}}.$$

The *conditional* notation $|$ is used in defining the partial correlation since the partial correlation is equivalent to *conditional correlation* if $\mathbb{E}(Y|X) = \mathbf{a} + BX$ for some vector \mathbf{a} and matrix B , which is true under the normality of data. This is the formulation we used to compute the partial correlation. If vector X consists of a single measurement, i.e. $X = X_1$, the partial correlation can be computed from the simple correlation via

$$\rho_{Y_1, Y_2|X} = \frac{\rho_{Y_1, Y_2} - \rho_{Y_1, X}\rho_{Y_2, X}}{\sqrt{(1 - \rho_{Y_1, X}^2)(1 - \rho_{Y_2, X}^2)}}.$$

The *sample partial correlation* $r_{Y_1, Y_2|X}$ is defined similarly by replacing the covariance with the sample covariance in (2).

If we let ρ_k be the partial correlation for group k (autism = 1, control = 2), for each fixed $p \in \partial\Omega$, one may test

$$H_0^A : \rho_k(p) = 0 \text{ vs. } H_1^A : \rho_k(p) \neq 0. \quad (3)$$

Inference type (3) is useful if only one sample is available or determining high correlation regions within a group. Assuming the normality of measurements X and Y , the partial correlation $r = r_{Y_i, Y_j | X}$ can be transformed to be distributed as:

$$T = \frac{r\sqrt{n-2}}{\sqrt{1-r^2}} \sim t_{n-2},$$

the t distribution with $n - 2$ degrees of freedom. This test statistic can be used for testing a one-sample inference type (3).

The MATLAB codes for computing the partial correlation are given here. Let `rho` be the sample partial correlation between cortical thickness (`thick`) and response time (`time`) while removing the effect of age (`age`) and cortical area (`area`) difference in a group at a single vertex. For n subjects in the group, all variables are row vectors of size $1 \times n$. The MATLAB codes for computing `rho` is as follows:

```
x=[age; area];
y=[thick; time];
a=cov([x;y]');
b=a(1:2,1:2)-a(1:2,3:4)*inv(a(3:4,3:4))*a(3:4,1:2);
rho=b(1,2)/sqrt(b(1,1)*b(2,2));
```

Here x and y are $2 \times n$ matrices, and the covariance matrix a is the size 4×4 .

3. Surface-based Data Smoothing

To increase the signal-to-noise ratio, we applied a surface based smoothing method called *heat kernel smoothing* to the cortical thickness measures. The implementation detail and its statistical properties can be found in Chung et al. (2005). This is an improved formulation over the previously developed *diffusion smoothing* (Andrade et al., 2001; Chung et al., 2003; Cachia et al., 2003). In Andrade *et al.* (2001) and Cachia *et al.* (2003), smoothing is done by solving an isotropic heat equation via the combination of the least squares estimation of the Laplace-Beltrami operator and the finite difference method (FDM). In Chung *et al.* (2003), the heat equation is solved using

the finite element method (FEM) and a similar FDM. The problem with these approaches to data smoothing is the complexity of setting up the FEM and making the FDM converge. Our heat kernel smoothing avoids all these problems.

We assume the following linear model on thickness measure Y :

$$Y(\mathbf{p}) = \theta(\mathbf{p}) + \epsilon(\mathbf{p}),$$

where $\theta(\mathbf{p})$ is the unknown mean thickness function and $\epsilon(\mathbf{p})$ is a zero-mean random field, possibly a Gaussian white noise process. Heat kernel smoothing of cortical thickness Y is then defined as the convolution:

$$K_\sigma * Y(\mathbf{p}) = \int_{\partial\Omega} K_\sigma(\mathbf{p}, \mathbf{q}) Y(\mathbf{q}) \, d\mathbf{q}, \quad (4)$$

where K_σ is the heat kernel that generalizes the Gaussian kernel in a Euclidean space to a curved manifold. The bandwidth σ controls the amount of smoothing. Given the Laplace-Beltrami operator $\Delta\psi = \lambda\psi$ on $\partial\Omega$, we can order eigenvalues $0 = \lambda_0 \leq \lambda_1 \leq \lambda_2 \leq \dots$ and corresponding eigenfunctions ψ_0, ψ_1, \dots . It can be written in terms of basis function expansion:

$$K_\sigma * Y(\mathbf{p}) = \sum_{j=0}^{\infty} Y_j e^{-\lambda_j \sigma} \psi_j(\mathbf{p}),$$

where

$$Y_j = \int_{\partial\Omega} \psi_j(\mathbf{q}) Y(\mathbf{q}) \, d\mathbf{q}.$$

The *heat kernel estimator* of unknown functional signal $\theta(\mathbf{p})$ is then

$$\hat{\theta}_\sigma(\mathbf{p}) = K_\sigma * Y(\mathbf{p}).$$

The heat kernel estimator becomes unbiased as $\sigma \rightarrow 0$, i.e.

$$\lim_{\sigma \rightarrow 0} \mathbb{E} \hat{\theta}_\sigma(\mathbf{p}) = \theta(\mathbf{p}).$$

As σ gets larger, the bias increases. However the total bias over all cortex is always zero, i.e. $\int_{\partial\Omega} [\theta(\mathbf{p}) - \mathbb{E} \hat{\theta}_\sigma(\mathbf{p})] \, d\mathbf{p} = 0$. Further

$$\lim_{\sigma \rightarrow \infty} \hat{\theta}_\sigma(\mathbf{p}) = \frac{\int_{\partial\Omega} Y(\mathbf{q}) \, d\mathbf{q}}{\int_{\partial\Omega} d\mathbf{q}},$$

the sample mean over the whole cortex $\partial\Omega$. Other properties of the heat kernel smoothing can be found in Chung et al. (2005). The heat kernel smoothing has been implemented in MATLAB and it can be found in the web www.stat.wisc.edu/~mchung/software/hk/hk.html. The approximate relationship between the full width at half maximum (FWHM) and the bandwidth is

$$\text{FWHM} = \sqrt{8 \ln 2} \sigma.$$

In this study, the thickness measurements were smoothed with 30 mm FWHM. This is the same amount of smoothing previously used in Chung et al. (2005) for detecting cortical thinning in autism.

4. Statistical Inference

In our study, the main interest is testing the equality of correlations between groups. So at each fixed point $\mathbf{p} \in \partial\Omega$, we are interested in testing

$$H_0^B : \rho_1(\mathbf{p}) = \rho_2(\mathbf{p}) \text{ vs. } H_1^B : \rho_1(\mathbf{p}) \neq \rho_2(\mathbf{p}). \quad (5)$$

For two sample inference type (5), one approach is based on the *Fisher transform* (Fisher, 1915; Hawkins, 1989; Bond and Richardson, 2004), which shows the asymptotic normality:

$$r_k \rightarrow \text{arctanh}(r_k) = \frac{1}{2} \ln \left(\frac{1+r_k}{1-r_k} \right) \sim N \left(\frac{1}{2} \ln \left(\frac{1+\rho_k}{1-\rho_k} \right), \frac{1}{n_k-3} \right).$$

The transform can be viewed as a variance stabilizing normalization process. Based on the Fisher transform, the test statistic under H_0^B is then given by:

$$W(\mathbf{p}) = \frac{\ln \left(\frac{1+r_1}{1-r_1} \cdot \frac{1-r_2}{1+r_2} \right)}{2 \sqrt{\frac{1}{n_1-3} + \frac{1}{n_2-3}}} \sim N(0, 1). \quad (6)$$

A slightly different formulation for testing the equality of correlations can be found in Crawford et al. (2003). We further normalized the field $W(\mathbf{p})$ with mean $\mu(\mathbf{p}) = \mathbb{E}W(\mathbf{p})$ and variance $S^2(\mathbf{p}) = \mathbb{E}W^2(\mathbf{p}) - \mu^2(\mathbf{p})$ by

$$Z(\mathbf{p}) = \frac{W(\mathbf{p}) - \mu(\mathbf{p})}{S(\mathbf{p})}.$$

μ and S^2 are estimated from random permutations. We can take the field Z to be Gaussian with zero mean and unit variance. To determine the null

distribution of the test statistic, we permute two samples across the groups. For n_1 subjects for group 1 and n_2 subjects for group 2, we combine them together, do a random permutation, and partition the result into two groups with the same number of subjects. For this study, we generated 200 random permutations out of $(n_1 + n_2)!$ possible permutations. Then for each permutation, we computed the statistic and based on the empirical distribution of the statistic, we estimated μ and S^2 .

Using Z as the test statistic, we tested:

$$\begin{aligned} H_0 : \rho_1(p) &= \rho_2(p) \text{ for all } p \in \partial\Omega \text{ vs.} \\ H_1 : \rho_1(p) &\neq \rho_2(p) \text{ for some } p \in \partial\Omega. \end{aligned}$$

The null hypothesis H_0 is the intersection of collection of hypotheses

$$H_0 = \bigcap_{p \in \partial\Omega} H_0^B(p),$$

where H_0^B is the null hypothesis given in (5). The type I error α for testing one sided test is then given by:

$$\begin{aligned} \alpha &= P\left(\bigcup_{p \in \partial\Omega} \{Z(p) > h\}\right) \\ &= 1 - P\left(\bigcap_{p \in \partial\Omega} Z(p) \leq h\right) \\ &= 1 - P\left(\sup_{p \in \partial\Omega} Z(p) \leq h\right) \\ &= P\left(\sup_{p \in \partial\Omega} Z(p) > h\right) \end{aligned}$$

for some h . The distribution of $\sup_{p \in \partial\Omega} Z(p)$ is asymptotically given as:

$$P\left(\sup_{p \in \partial\Omega} Z(p) > h\right) \approx \sum_{d=0}^2 \phi_d(\partial\Omega) \rho_d(h), \quad (7)$$

where ϕ_d are the d -dimensional Minkowski functionals of $\partial\Omega$ and ρ_d are the d -dimensional Euler characteristic (EC) density of correlation field (Worsley et al., 1995). The Minkowski functionals are $\phi_0 = 2, \phi_1 = 0, \phi_2 =$

$\text{area}(\partial\Omega)/2 = 49,616\text{mm}^2$, the half area of the template cortex $\partial\Omega$. The EC densities are:

$$\begin{aligned}\rho_0(h) &= \int_h^\infty \frac{1}{\sqrt{2\pi}} e^{-u^2/2} du \\ \rho_1(h) &= \frac{(4 \ln 2)^{1/2}}{2\pi\text{FWHM}} e^{-h^2/2} = \frac{1}{2\sqrt{2}\pi\sigma} e^{-h^2/2} \\ \rho_2(h) &= \frac{1}{(8\pi)^{3/2}\sigma^2} h e^{-h^2/2} = \frac{4 \ln 2}{(2\pi)^{3/2}\text{FWHM}^2} h e^{-h^2/2}.\end{aligned}$$

The resulting P-value maps are found in Figure 1 and 2.

5. Application

We applied our methodology to detect the regions of abnormal brain-behavior correlates in autistic cortical regions.

Subjects. 14 high functioning autistic (HFA) and 12 normal control (NC) subjects used in this study were screened to be right-handed males. Age distributions for HFA and NC are 15.93 ± 4.71 and 17.08 ± 2.78 respectively. This is the same data set used in previous studies Chung, et al. (2004), Chung, et al. (2005) and Dalton, et al. (2005).

Magnetic resonance images. High resolution anatomical magnetic resonance images (MRI) were obtained using a 3-Tesla GE SIGNA (General Electric Medical Systems, Waukesha, WI) scanner with a quadrature head RF coil. A three-dimensional, spoiled gradient-echo (SPGR) pulse sequence was used to generate T_1 -weighted images. The imaging parameters were $\text{TR}/\text{TE} = 21/8$ ms, flip angle = 30° , 240 mm field of view, 256×192 in-plane acquisition matrix (interpolated on the scanner to 256×256), and 128 axial slices (1.2 mm thick) covering the whole brain.

Cortical thickness. Following image processing steps described in Chung, et al. (2004) and Chung, et al. (2005) both the outer and inner cortical surfaces were extracted for each subject via deformable surface algorithm (MacDonald et al., 2000). Surface normalization is performed by minimizing an objective function that measures the global fit of two surfaces while maximizing the smoothness of the deformation in such a way that the pattern

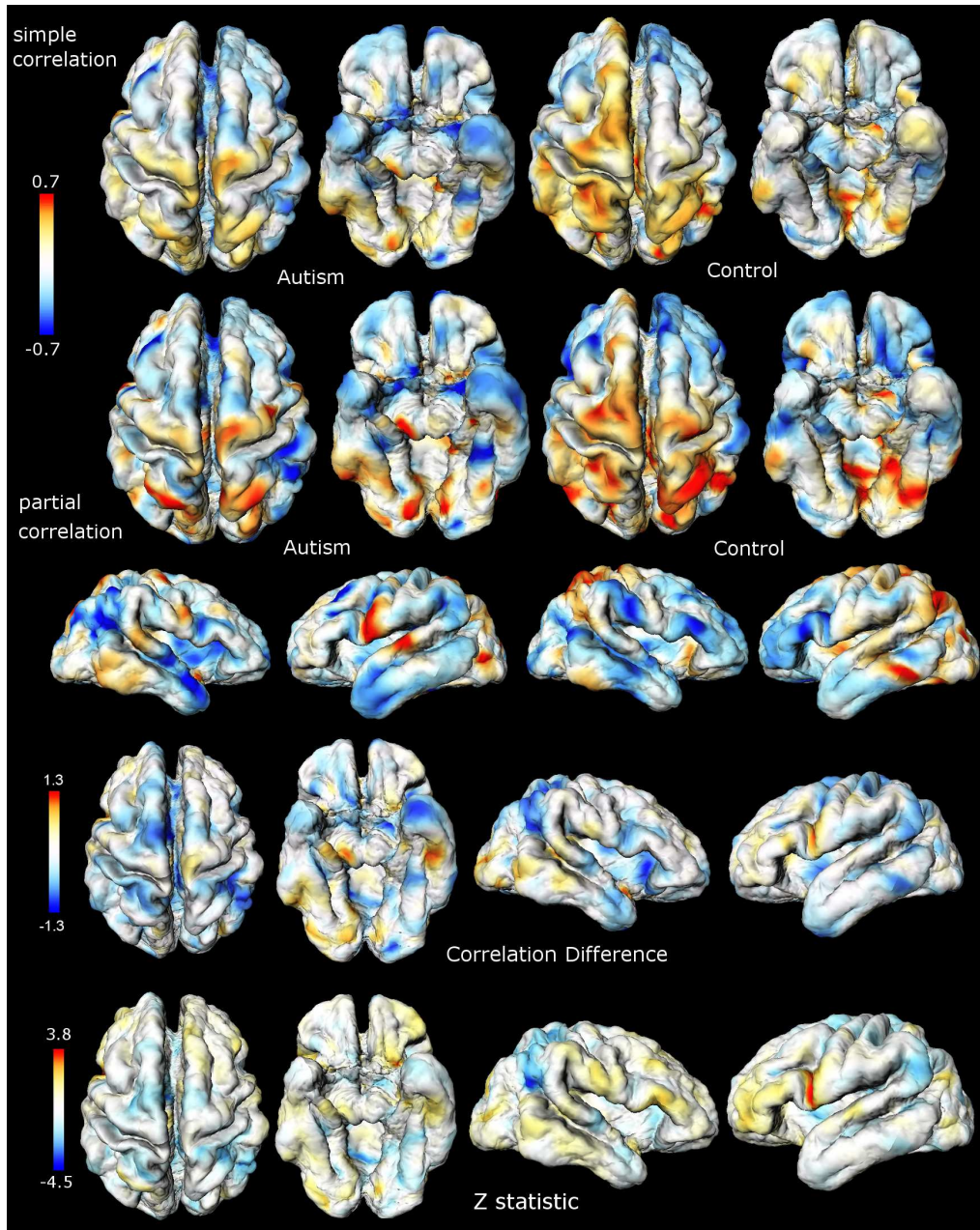


Figure 1: Map of facial emotion discrimination task score correlated with thickness. The first row is the simple correlation. The second and third rows are the partial correlation. The partial correlation tend to boost over all correlation values. The fourth row is the partial correlation difference between the two groups (autism – control). The last row shows the final Z-statistic map showing statistically significant correlation difference (P-value 0.03 for $z = 3.8$, and 0.002 for $z = -4.5$).

of gyral ridges are matched smoothly (Robbins, 2003; Chung et al., 2005). Afterward cortical thickness was computed for each subject (Chung et al., 2003; Chung et al., 2005). Heat kernel smoothing was applied to the cortical thickness measures with a relatively large 30mm FWHM as described in a previous section.

Facial emotion discrimination task. The subjects were asked to decide whether a picture of a human face was either emotional (happiness, fear or anger) or neutral (showing no obvious emotion) by pressing one of two buttons. The faces were black and white photographs taken from the Karolinska Directed Emotional Faces set (Lundqvist, et al., 1988; Dalton, et al., 2005). The task scores (maximum 40) for HFA and NC are 27.14 ± 15.34 and 39.42 ± 0.79 respectively, and the response time (ms) for HFA and NC are 1329.8 ± 206.7 and 1110.9 ± 182.3 and respectively. A more detailed description about the task can be found in Dalton et al. (2005).

Partial correlation maps. The simple correlations between cortical thickness and both task score and response time were computed for each group and mapped onto the template cortex (Figure 1 and 2, first rows). The partial correlations were also computed while removing the effect of age and global area difference. (Figure 1 and 2, second and third rows). Comparing the partial correlation maps to the simple correlation maps, we see different patterns indicating that it is necessary to account for the age and the area terms for proper correlation analysis. The partial correlation difference maps (autism – control) show the regions of maximum correlation difference (Figure 1 and 2, fourth rows). To access the statistical significance of the correlation difference, the Fisher transformation and the normalization steps were used resulting in the Z-statistic maps (Figure 1 and 2, last rows).

Group difference between the autistic and control subjects were identified using brain-behavior correlations of task score and response time. Brain-behavior partial correlations of task score and cortical thickness identified group differences in mainly two cortical regions: right angular gyrus (area 39) and the left Broca’s area (area 44). The area 39 shows the positive correlation for the control subjects while it shows the negative correlation for the autistic subjects (corrected P-value 0.002, z-value -4.5). The area 44 shows the negative correlation for the control subjects while it shows the positive correlation for the autistic subjects (corrected P-value of 0.03, z-value 3.8).

For time-thickness correlation, we found more statistically significant regions of difference that are consistent with previous studies. In general, the spatial patterns of behavioral response time and thickness correlation shows more negative correlation (blue) than positive correlation (red) in the control subjects and the pattern is opposite for the autistic subjects (Figure 2 second row). Faster response time in the control subject are related to a thicker right ventral and dorsal prefrontal cortex while they are related to thinning in the same area in the autistic subject (corrected P-value 0.001, z-value 4.6). We found correlation difference in the left superior temporal gyrus and superior temporal sulcus (corrected P-value 0.04, z-value -3.7) (Figure 2 last row). The autistic subjects show an aberrant spatial pattern of behavioral-thickness correlation in the right frontopolar region (BA10), which shows a direct correlation between response time duration and cortical thickness not seen in the control subjects. We also found that slower responses in controls are related to a thinner right inferior orbital frontal cortex but slower responses in the autistic subject are independent of right orbital prefrontal cortical thickness (corrected P-value 0.001, z-value 4.6).

6. Discussions

In this study, group difference between the autistic and the control subjects were identified using brain-behavior correlations between cortical thickness and both task score and response time. The partial correlation mapping strategy is shown to be an effective way of visualizing and localizing the cortical regions of high correlation while removing the effect of unwanted covariates such as age, gender and global brain size differences. Our approach would be a very useful analysis framework for many other types of future brain-behavior correlate studies.

Our findings are consistent with previous functional and anatomical studies. The score-thickness correlation difference found in the left area 44 is interesting since this is the area shown to have reduced bilateral connectivity in autism (Villalobos et al., 2005). Since area 44 is thought to contain mirror neurons considered part of the dorsal stream, altered brain-behavior correlations reflect the influence of cortical thickness on perception-action function (Rizzolatti et al., 2002; Villalobos et al., 2005).

The ventral prefrontal plays a role in the learning of tasks in which subjects must learn to associate visual cues and responses (Passingham et al., 2000; Passingham and Toni, 2001). So our finding of abnormal correlation

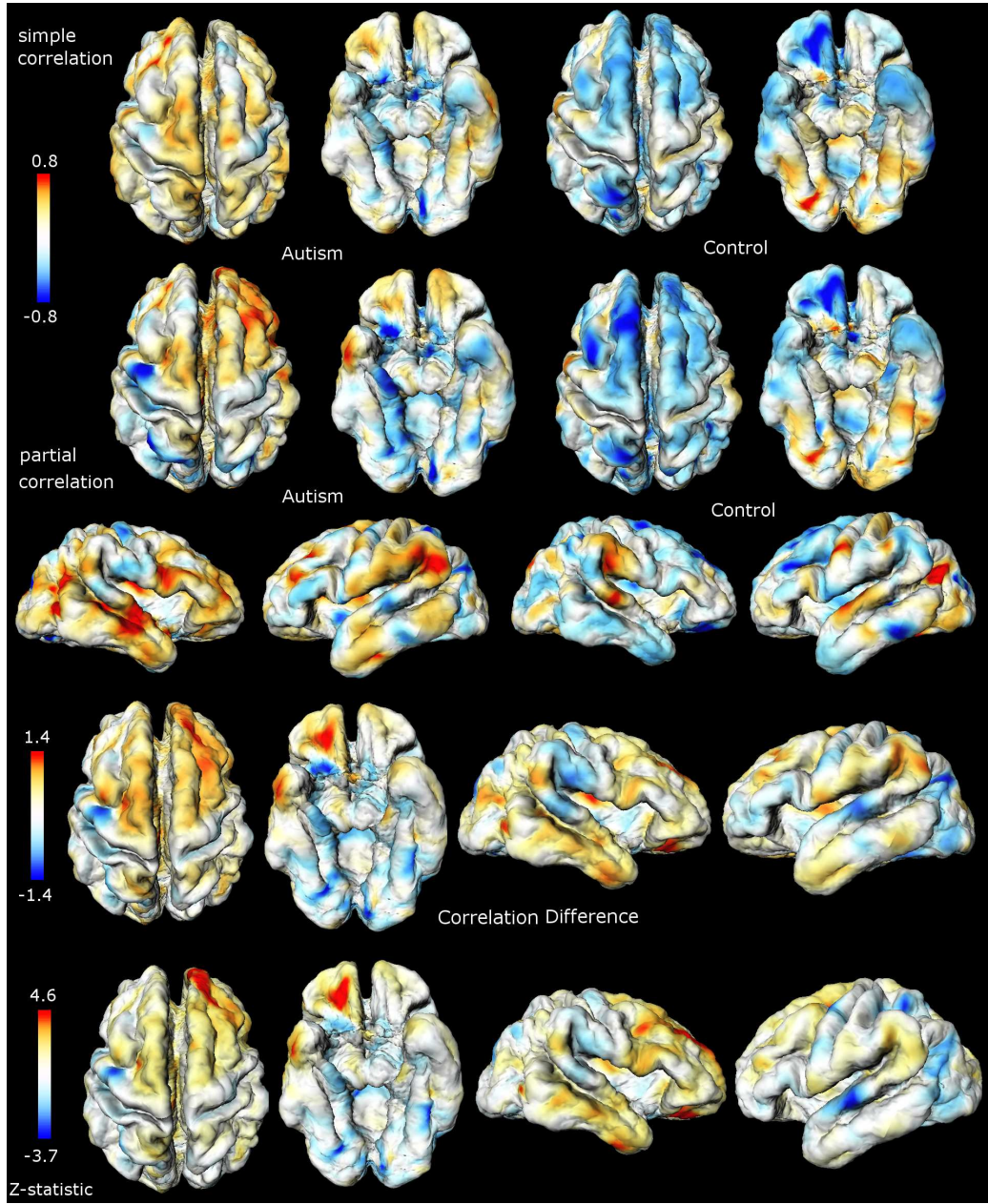


Figure 2: Map of response time correlated with thickness. The first row shows the simple correlation. The second and third rows are the partial correlation removing the effect of age and cortical area differences. The fourth row shows the partial correlation difference. We are interested in testing the significance of this difference. The last row shows the final Z-statistic map showing statistically significant correlation difference (corrected P-value 0.04 for $z = -3.7$ and 0.001 for $z = 4.6$).

between the response time and thickness in the right ventral prefrontal cortex is not surprising.

Our previous study identified reduced cortical thickness in the right inferior orbital prefrontal cortex, the left superior temporal sulcus and the left occipito-temporal gyrus in the autistic subjects relative to the control group (Chung et al., 2005). When paired with results from our current study, areas in which cortical thickness is reduced in autism predict differences in task response. Thicker cortex in the left superior temporal gyrus and the superior temporal sulcus predict faster response times in the control subjects, whereas thicker cortex in the autistic subject are associated with prolonged response times in these regions. This result may be related to autistic dysfunction in the superior temporal gyrus and superior temporal sulcus, regions known to be involved in social processing (Baron-Cohen et al., 1999; Allison et al., 2000) and eye gaze perception (Hooker et al., 2003). Slower responses in controls are related to a thinner right inferior orbital frontal cortex but slower responses in the autistic subject are independent of right orbital prefrontal cortical thickness. This may suggest a floor effect in which autistic cortical thickness is too thin to predict changes in behavioral response time.

The general spatial patterns of behavioral response time-thickness correlations distributed across the dorsal surface are positive in the autistic subjects, whereas negative correlations are shown for the control subjects in these regions. Autistics also show an aberrant spatial pattern of behavioral-thickness correlation in the right frontopolar region (BA10), which shows a direct correlation between response time duration and cortical thickness not seen in controls. One possible mechanism for these results is that increased cortical thickness may produce alterations in intra cortical connectivity resulting in a mis-allocation of cortical functional resources. A recent study suggesting that alterations are noted along the thickness of autistic cortex further complicates the impact that alterations in autistic cortical anatomy may have on behavior. Based on cellular studies, autistic subjects have an increased number of smaller mini-columns, the basic functional unit of cortex (Buxhoeveden and Casanova, 2002), that are less compact relative to control subjects in prefrontal cortex and in temporal regions. This anatomy may increase intracortical signalling, reduce lateral inhibition, and cause terminal fields of subcortical afferents to synapse on multiple mini-columns unintentionally enhancing cortical noise in these regions (Casanova et al., 2002). Our results add to this literature by identifying regions in which cortical thickness alterations predict certain autistic behaviors.

References

1. Andrade, A., Kherif, F., Mangin, J., Worsley, K.J., Paradis, A., Simon, O., Dehaene, S., Le Bihan, D., Poline, J-B. 2001. Detection of fMRI activation using cortical surface mapping, *Human Brain Mapping* 12, 79-93.
2. Allison, T., Puce, A., McCarthy, G. 2000. Social perception from visual cues: role of the STS region.
3. Baron-Cohen, S., Ring, H.A., Wheelwright, S., Bullmore, E.T., Brammer, M.J., Simmons, A., Williams, S. C. R. 1999. Social intelligence in the normal and autistic brain: an fMRI study. *European Journal of Neuroscience* 11, 1891-1898.
4. Buxhoeveden, D.P., Casanova, M.F. 2002. The minicolumn hypothesis in neuroscience. *Brain* 125, 935-951.
5. Bond, C.F., Richardson, K. 2004. Seeing the Fisher Z-transformation. *Psychometrika* 60, 291-303.
6. Cachia, A. and Mangin, J.-F. and Rivière, D., Papadopoulos-Orfanos, D. and Kherif, F. and Bloch, I., Régis, J. 2003. A generic framework for parcellation of the cortical surface into gyri using geodesic Voronoi diagrams, *Medical Image Analysis* 7, 403-416.
7. Cao, J. and Worsley, K.J. 1998. The geometry of correlation fields with an application to functional connectivity of the brain. *Annals of Applied Probability*, 9, 1021-1057.
8. Casanova, M.F., Buxhoeveden, D.P., Switala, A.E., Roy, E. 2002. Minicolumnar pathology in autism. *Neurology*, 58:428-432.
9. Chung, M.K., Worsley, K.J., Robbins, S., Paus, P., Taylor, J., Giedd, J.N., Rapoport, J.L., Evans, A.C. 2003. Deformation-based surface morphometry applied to gray matter deformation, *NeuroImage* 18, 198-213.
10. Chung, M.K., Dalton, K.M., Alexander, A.L., Davidson, R.J. 2004. Less white matter concentration in autism: 2D voxel-based morphometry. *NeuroImage* 23, 242-251.
11. Chung, M.K., Robbins, S., Dalton, K.M., Davidson, R.J., Alexander, A.L., Evans, A.C. 2005. Cortical thickness analysis in autism via heat kernel smoothing. *NeuroImage* 25, 1256-1265.
12. Crawford, J.R., Garthwaite, P.H., Howell, D.C., Venner, A. 2003. Intra-individual measures of association in neuropsychology: inferential meth-

- ods for comparing a single case with a control or normative sample. *Journal of the International Neuropsychological Society*. 9, 989-1000.
13. Dalton, K.M., Nacewicz, B.M., Johnstone, T., Schaefer, H.S., Gernsbacher, M.A., Goldsmith, H.H., Alexander, A.L., Davidson, R.J. 2005. Gaze fixation and the neural circuitry of face processing in autism. *Nature Neuroscience* 8, 519-526.
 14. Friston, K.J., Frith, C.D., Liddle, P.F., Frackowiak, R.S.J. 1993. Functional connectivity: The principal-component analysis of large (PET) data sets. *Journal of Cerebral Blood Flow and Metabolism*, 13:5-14
 15. Friston, K.J., Frith, C.D., Fletcher, P., Liddle, P.F., Frackowiak, R.S.J. 1996. Functional Topography: Multidimensional Scaling and Functional Connectivity in the Brain Cerebral Cortex. *Cerebral Cortex*. 6, 156-164.
 16. Fisher, R.A. 1915. Frequency distribution of the values of the correlation coefficient in samples of an indefinitely large population. *Biometrika*, 10, 507-521.
 17. Hawkins, D.L. 1989. Using U statistics to derive the asymptotic distribution of Fisher's Z statistic. *The American Statistician*, 43, 235-237.
 18. Horwitz, B., Grady, C.L., Mentis, M.J., Pietrini, P., Ungerleider, L.G., Rapoport, S.I., Haxby, J.V. 1996. Brain functional connectivity changes as task difficulty is altered. *NeuroImage*, 3:S248.
 19. Hooker, C.I., Paller, K.A., Gitelman, D.R., Parrish, T.B., Mesulam, M.-M., Reber, P.J. 2003. Brain networks for analyzing eye gaze. *Cognitive Brain Research*. 17, 406-418.
 20. Lundqvist, D., Flykt, A., Ohman, A. 1998. Karolinska directed emotional faces. Department of Neurosciences, Karolinska Hospital, Stockholm, Sweden.
 21. MacDonald, J.D., Kabani, N., Avis, D., Evans, A.C. 2000. Automated 3-D Extraction of Inner and Outer Surfaces of Cerebral Cortex from MRI. *NeuroImage*, **12**:340-356.
 22. Passingham, R.E., Toni, I., Rushworth, M.F.S. 2000. Specialisation within the prefrontal cortex: the ventral prefrontal cortex and associative learning. *Exp. Brain Res.* 133, 103-113.
 23. Passingham, R.E., Toni, I. 2001. Contrasting the dorsal and ventral visual systems: guidance of movement versus decision making. *NeuroImage* 14:S124-31.

24. Rizzolatti, G., Fogassi, L., Gallese, V. 2002. Motor and cognitive functions of the ventral premotor cortex. *Cognitive Neuroscience*. 12, 149-154.
25. Robbins, S.M. 2003. Anatomical Standardization of the Human Brain in Euclidean 3-Space and on the Cortical 2-Manifold. PhD thesis, School of Computer Science, McGill University, Montreal, QC, Canada.
26. Thompson, P.M., Cannon, T.D., Narr, K.L., van Erp, T., Poutanen, V.P., Huttunen, M., Lonnqvist, J., Standertskjold-Nordenstam, C.G., Kaprio, J., Khaledy, M., Dail, R., Zoumalan, C.I., Toga, A.W. 2001. Genetic influences on brain structure. *Nature Neuroscience*. 12, 1253-1258.
27. Villalobos, M.E., Mizuno, A., Dahl, B.C., Kemmotsu, N., Muller, R.-A. 2005. Reduced functional connectivity between V1 and inferior frontal cortex associated with visuomotor performance in autism.
28. Worsley, K.J., Marrett, S., Neelin, P., Evans, A.C. 1995. A unified statistical approach for determining significant signals in location and scale space images of cerebral activation. Quantification of brain function using PET, Eds. R. Myers, V.J.Cunningham, D.L. Bailey and T. Jones , Academic Press, San Diego, 327-333.
29. Worsley, K.J., Cao, J., Paus, T., Petrides, M., Evans, A.C. 1998. Applications of random field theory to functional connectivity. *Human Brain Mapping*, 6, 364-367.
30. Worsley, K.J., Charil, A., Lerch, J., Evans, A.C. 2005. Connectivity of anatomical and functional MRI data. The Proceeding of the International Joint Conference on Neural Networks, Montreal, Quebec, Canada.